Carbonates from the ancient world's longest aqueduct

Received: 14 July 2020 | Revised: 30 December 2020 | Accepted: 16 February 2021

DOI: 10.1002/gea.21853

RESEARCH ARTICLE

Geoarchaeology An International Journal WILEY

Carbonates from the ancient world's longest aqueduct: A testament of Byzantine water management

Gül Sürmelihindi[1] | Cees Passchier[1] | James Crow[2] | Christoph Spötl[3] | Regina Mertz-Kraus[1]

[1]Institute for Geosciences, Johannes Gutenberg University of Mainz, Mainz, Germany

[2]School of History, Classics and Archaeology, University of Edinburgh, Edinburgh, UK

[3]Institute of Geology, University of Innsbruck, Innsbruck, Austria

Correspondence
Gül Sürmelihindi, Institute for Geosciences, Johannes Gutenberg University of Mainz, Mainz, Germany.
Email: surmelih@uni-mainz.de

Scientific editing by Stathis Stiros

Funding information
Leverhulme Trust; Deutsche Forschungsgemeinschaft

Abstract

The fourth- and fifth-century aqueduct system of Constantinople is, at 426 km, the longest water supply line of the ancient world. Carbonate deposits in the aqueduct system provide an archive of both archaeological developments and palaeo-environmental conditions during the depositional period. The 246-km-long aqueduct line from the fourth century used springs from a small aquifer, whereas a 180-km-long fifth-century extension to the west tapped a larger aquifer. Although historical records testify at least 700 years of aqueduct activity, carbonate deposits in the aqueduct system display less than 27 years of operation. This implies that the entire system must have been cleaned of carbonate, presumably during regular campaigns. A 50-km-long double-aqueduct section in the central part of the system may have been a costly but practical solution to allow repairs and cleaning of the aqueducts of carbonate to ascertain a continuous water supply to the city. The fifth-century channel was commonly contaminated with clay, caused by the nature of the aqueduct system and possible local damage to the channel. This clay-rich water could have been one of the reasons for the construction of large reservoirs in Constantinople.

KEYWORDS

Byzantine, carbonate, Constantinople, Roman aqueduct, water supply

1 | INTRODUCTION

Roman aqueducts are among the greatest technological and cultural achievements of classical antiquity and represent an important development for society (Hodge, 2011; Oleson, 1984). Where these aqueducts were fed by karstic water sources, calcium carbonate commonly formed in the channels and can be used to reconstruct patterns of water discharge, temperature and chemical composition in antiquity (Passchier, Sürmelihindi, & Spöt, 2016a; Sürmelihindi, & Spöt, Mertz-Kraus et al., 2016b; Sürmelihindi, Passchier, Baykan et al., 2013; Sürmelihindi, Passchier, Spötl et al., 2013). Carbonate deposits in ancient water systems, therefore, constitute an important archive of environmental, climatic and operational conditions. However, if the deposition rate was high, carbonate accumulation could also block an aqueduct channel in a short time, and therefore *Frontinus*[1] (AD 30–103) already advised the regular removal of such

deposits. Some aqueducts indeed show evidence of periodic cleaning and maintenance (Kienast, 1995; Passchier et al., 2015). We studied carbonate deposits from the main aqueducts of the Byzantine capital of Constantinople, the longest aqueduct of the ancient world (Çeçen, 1996), to determine how this system was built, used and maintained. Our aim was to understand how the environmental setting played a role in the city's multistage water management, and if any arrangement was made for removal of carbonate from the channels or for maintenance work in response to natural hazards such as earthquakes or floodwater.

1.1 | Aqueducts of Constantinople

When Constantinople was founded in AD 330 as the new capital for the Roman Empire, it inherited a Hadrianic water system that was originally designed for the predecessor city of *Byzantium* at the same location (Figure 1; Mango, 1995). This aqueduct system, with 47-km length, started in the Belgrad Forest in hills to the north of the city and provided the lower parts of the city with water, but could not supply its new, upper reaches (Crow, 2019, p. 214; Snyder, 2012, p. 199). The new city of Constantinople, therefore, required an extensive new water system, which was built on a grand scale in two phases (Figures 1 and 2). The first phase was built in the mid-late fourth century[2] during the reign of the Emperors Constantius II, Julian and Valens using three springs at Danamandıra and several springs at Pınarca, in two branches that joined near Kalfaköy (Figures 1 and 2a; Crow et al., 2008, p. 52; Crow, 2019; Ruggeri, 2018, pp. 51–53). These springs were fed by a small aquifer in Eocene limestone of the Soğucak formation (Lom et al., 2016; Varol et al., 2009). The second phase was built in the early fifth century, extending the aqueduct system to the high-discharge springs of Pazarlı, 120 km from the city in a straight line, with additional springs in the Ergene Valley near Ayvacık and at Binkılıç (Figures 1 and 2a). These springs are fed from a larger aquifer in the same Eocene formation. The last 50 km of the fifth-century aqueduct extension ran parallel to the Kaynarca branch of the fourth-century system, from the Ballıgerme bridge (K18; Figures 2a and 3a)[3] at least to Kalfaköy (Figure 2, double section). It is still unknown if the fifth-century extension ran all the way to the city, parallel to the fourth-century aqueduct, or joined the fourth-century line near Kalfaköy: the latter seems most likely, but the matter remains unresolved (Figure 2). The entire water system[4] was designed using masonry channels with an arched vault, internally plastered with standard waterproof *opus signinum* cement (Figure 3e-g). The channels were supported by over 90 bridges and by several tunnels up to 5 km long (Figure 3a-c; Crow, in press; Crow, 2019; Crow et al., 2008). The aqueducts fed several large cisterns in the city and three huge open reservoirs[5], with a combined storage capacity of 900.000 m^3 (Ruggeri, 2018, p. 35, 244; Ward et al., 2017). In the fourth and fifth centuries, Roman engineers already had half a millennium of experience in the construction of water supply systems, but the Constantinople system was still a challenge due to its scale and the lack of nearby springs of sufficient discharge (Bono et al., 2001). Due to the hilly terrain, the actual length of the combined channels was at least 426 km, and maybe up to 565 km if a double channel ran all the way to the city (Çeçen, 1996; Crow, 2012; Crow et al., 2008; Ruggeri, 2018, p. 98). This implies that the combined aqueduct system is the longest and most complex water supply system for a city in the ancient world, both in Roman and Byzantine times (Çeçen, 1996). The system is only comparable in scale to the 11 aqueducts of Rome and to the large mining aqueduct system of Las Medulas in Spain (Matias Rodrigues, 2017), but is unique with respect to the length of its two individual channels.

The long-distance aqueduct system was apparently first cut in AD 487 by Theodoric Strabo in a civil war, but was repaired and then functioned till AD 626 when it was cut by the Avars during a siege of the city (Crow, 2019). A part of the system was only restored again by Constantine V in AD 765[6] (Crow, 2019; Crow et al., 2008, p. 236; Mango & Scott, 1997) and then functioned till the mid to late 12th century, when it was finally abandoned due to significant damage to the structure, notably the bridges (Crow et al., 2008; Ruggeri, 2018). After this time, the population of the city declined, and the original Hadrianic system would have been once again sufficient for the lower parts of the city, whereas the higher parts were fed by a new, more modest aqueduct system from the Halkalı springs (Figures 1 and 2a; Crow, 2019; Crow et al., 2008; Mango, 1995). These springs do not have a high discharge, and therefore would not have been sufficient to feed the early Byzantine city during its period of expansion when Constantinople was one of the largest cities in the world surpassing Rome (Crow, 2019, p. 212; Crow et al., 2008, p. 22; Mango, 1995, p. 10).

The slope of the two aqueduct channels is mostly between 0.7 and 0.9 m/km, and more gentle downstream from Kalfaköy (0.4–0.3 m/km; Figure 2b; Ruggeri, 2018, p. 99). The fifth-century channel starts at a higher level than the springs of the fourth-century channel, but descends rapidly, and lies 10 m *below* the fourth-century line at Ballıgerme, at the start of the double section (Figures 2b and 3a). The two channels then converge topographically and run parallel at different levels in the so-called 'double section' to reach a similar level by Kalfaköy, where they probably joined. In the double section (Figure 2b,c), the fourth- and fifth-century lines crossed streams either by separate bridges or by massive two-story structures such as the Kurşunlugerme and Kumarlıdere bridges

[1]Frontinus, De Aquis 121,122.

[2]Finished in AD 373 : Crow et al. (2008, p. 225).

[3]This bridge (Figure 3a) was unfortunately destroyed by treasure hunters using dynamite in February 2020 (https://arkeofili.com/istanbuldaki-tarihi-kemer-dinamitlerle-patlatildi/).

[4]The combined aqueduct system of fourth- and fifth-century channels is also referred to as the 'Valens aqueduct'. However, this can give rise to confusion with the Bozdoğan aqueduct bridge inside the old city of Constantinople (Figure 3c), which is also referred to as the 'Valens aqueduct' as a small part of the entire system.

[5]The Aetius Reservoir, built ca. AD 425 ; Aspar Reservoir, AD 459 and Mocius Reservoir AD 491–518? Ruggeri (2018, p. 35, 244) and Ward et al. (2017).

[6]Theophanes, Chronicle AM 6238 (translation Mango & Scott, 1997).

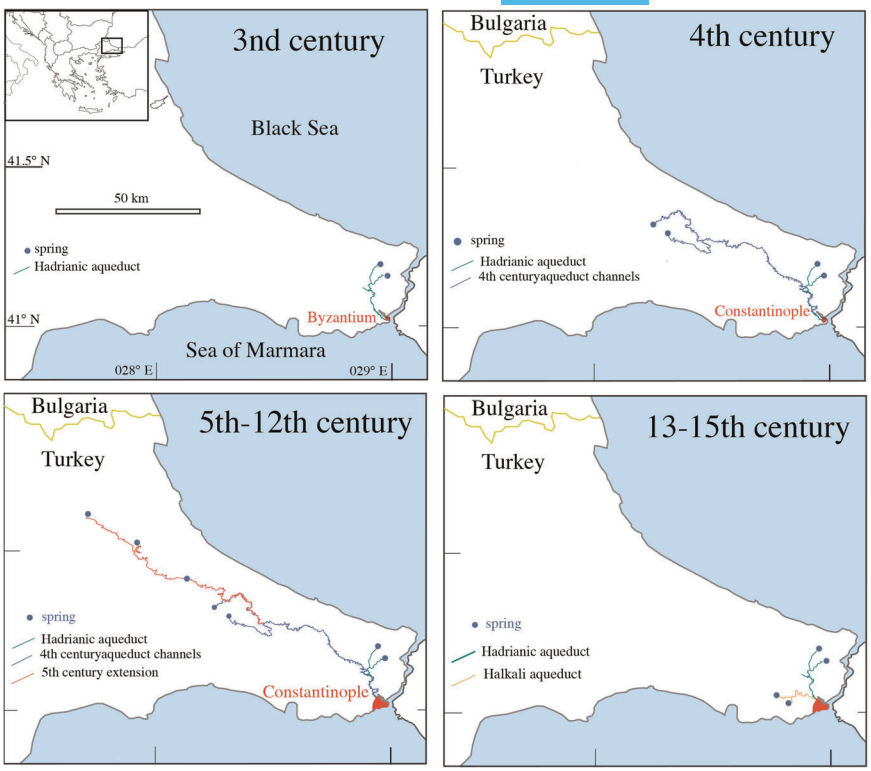

FIGURE 1 Development of the Constantinople water supply system during the late Roman and Byzantine period. Each diagram shows only the active water supply during a specific period [Color figure can be viewed at wileyonlinelibrary.com]

(Figure 3b; Crow, in press; Ruggeri, 2018). The channel segments had variable dimensions (Figure 3e-g; Ruggeri, 2018). The intake structure found in Pazarlı was possibly a dam in the Değirmendere stream, fed by karst springs (Çeçen, 1996; Crow et al., 2008; Ruggeri, 2018). Unlike covered spring catchment structures, such a dam increases the risk of clay contamination in times of storms. The intake at Pınarca was from three interconnected karstic springs emerging from small caves, some equipped with catchment installations such as basins and weirs to raise the water level (Figure 3d; Ruggeri, 2018, pp. 58–59). No structural information is presently available on the other spring catchments. The total capacity of the aqueducts delivering water to Constantinople was estimated at 0.7 m^3/s if the final stretch of channel is a single strand, and 2.07 m^3/s if the fourth- and fifth-century channels were separated all the way to the city (Ruggeri, 2018, p. 225). Due to their gentle slope, the flow speed was relatively low in the channels in the range of 0.5–1.0 m/s, and subcritical flow conditions prevailed throughout (Froude numbers of 0.2–0.4; Ruggeri, 2018, pp. 210–217).

1.2 | Carbonate deposits

Calcium carbonate deposits in ancient aqueducts are important archives of environmental and archaeological setting (Benjelloun et al., 2019; Passchier, Sürmelihindi, & Spötl, 2016a; Passchier, Sürmelihindi, Spötl, Mertz-Kraus et al., 2016b; Sürmelihindi, Passchier, Baykan et al., 2013; Sürmelihindi, Passchier, Spötl et al., 2013). Such deposits form when spring water supersaturated in calcium carbonate and with a high level of dissolved CO_2 is used to supply an aqueduct. Excess CO_2 degasses from water in the aqueduct channel and dissolved carbonate is then forced to settle on the channel walls and bottom. The resulting carbonate deposits are commonly layered due to seasonal changes in depositional conditions, similar to other freshwater carbonates such as tufa, travertine or speleothems (Pedley & Rogerson, 2010; Pentecost, 2005). Changes in water temperature and composition can be constrained from the analysis of stable isotopes ($\delta^{18}O$ and $\delta^{13}C$) and trace elements in the carbonate (Sürmelihindi, Passchier, Baykan et al., 2013; Sürmelihindi, Passchier, Spötl et al., 2013). $\delta^{18}O$ cyclicity can help to confirm the annual origin of layering and determine periods of usage (Benjelloun et al., 2019; Sürmelihindi et al., 2019). Although $\delta^{13}C$ is more challenging to understand, changes in biological activity in soil and channels, besides variations in precipitation and in vegetation cover of the aquifer, can be derived from $\delta^{13}C$ cyclicity (Passchier, Sürmelihindi, Spötl, Mertz-Kraus et al., 2016b; Sürmelihindi, Passchier, Baykan et al., 2013; Sürmelihindi, Passchier, Spötl et al., 2013). Discharge of an aqueduct can be deduced from layer thickness or from the combined slope, width and water level of the aqueduct (Hodge, 2011)[7].

2 | MATERIALS AND METHODS

Analytical work was done as outlined in our earlier studies on carbonate deposits in ancient water structures (Passchier, Sürmelihindi, & Spötl, 2016a; Passchier, Sürmelihindi, Spötl, Mertz-Kraus et al., 2016b;

[7]Water level in abandoned ancient aqueducts can be estimated from the height of carbonate on the channel walls, and discharge is calculated using the Gauckler–Manning equation (Hodge, 2011).

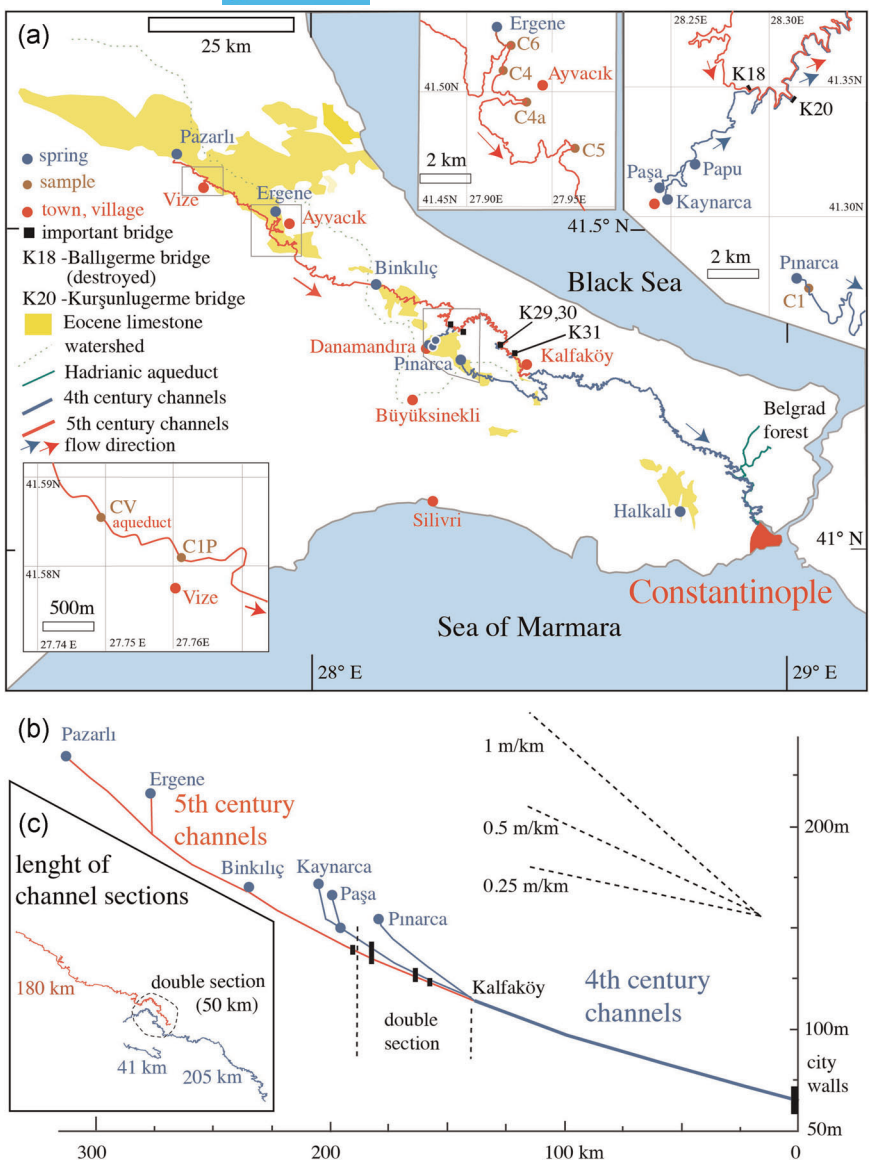

FIGURE 2 (a) Trace of the Hadrianic, fourth- and fifth-century aqueducts of Constantinople. Insets show enlarged maps of three locations discussed in the text and the locations where samples were collected. Limestone outcrops of the Eocene Soğucak formation, after Türkecan and Yurtsever (2002). Prominent bridges are marked as K18 to K31; (b) altitude profile of the aqueduct, after Ruggeri (2018). Black bars in the double section indicate bridges marked in (a) in the same sequence. (c) Schematic breakdown of the 426 km of the Valens aqueduct, separating the channel sections. Channel lengths, after Crow et al. (2008) and Ruggeri (2018). The location of the 50-km-long double section is indicated [Color figure can be viewed at wileyonlinelibrary.com]

Sürmelihindi, Passchier, Baykan et al., 2013, Sürmelihindi et al., 2019; Sürmelihindi, Passchier, Spötl et al., 2013). The samples were cut in half using a thin diamond saw. One slab was used to make polished thin sections and the other one was used for analyses. The microstructure and preferred orientation of calcite crystals were investigated by petrographic transmitted-light microscopy on thin sections. Thin sections were also scanned using a Fabric Analyser G60 (Peternell et al., 2009).

Stable oxygen and carbon isotope analyses were carried out at the University of Innsbruck. Polished slabs of all samples were micromilled at 0.2-mm intervals in traces 5 mm wide and parallel to the lamination. The sample powders were analysed using a semi-automated device (Gasbench II) linked to a ThermoFisher Delta V Plus isotope ratio mass spectrometer. Isotope values are reported on the VPDB scale and long-term precision is better than 0.1‰ for both $\delta^{13}C$ and $\delta^{18}O$ (Spötl & Vennemann, 2003).

Element distribution maps were produced using a JEOL JXA 8900 RL (JEOL) electron microprobe (EPMA) at the University of Mainz on carbon-coated thin sections. The instrument was operated at an acceleration voltage of 15 kV and a probe current of 26 nA. The spot size was 5 μm and the dwell time was 250 ms, with a step size of 30 or 3 μm for mapping the concentration distribution of Ca, Fe, Mg, Al, Si, Na and K. In this paper, only data from elements that show distinctive results are presented.

Measurements of trace element distribution were performed by laser ablation inductively coupled plasma mass spectrometry (LA-ICP-MS) using an ArF Excimer laser system (ESI NWR193) with an output wavelength of 193 nm coupled to an Agilent 7500ce ICP-MS. Details of the instrumentation and analytical parameters are described elsewhere (Passchier, Sürmelihindi, & Spötl, 2016a; Supporting Information).

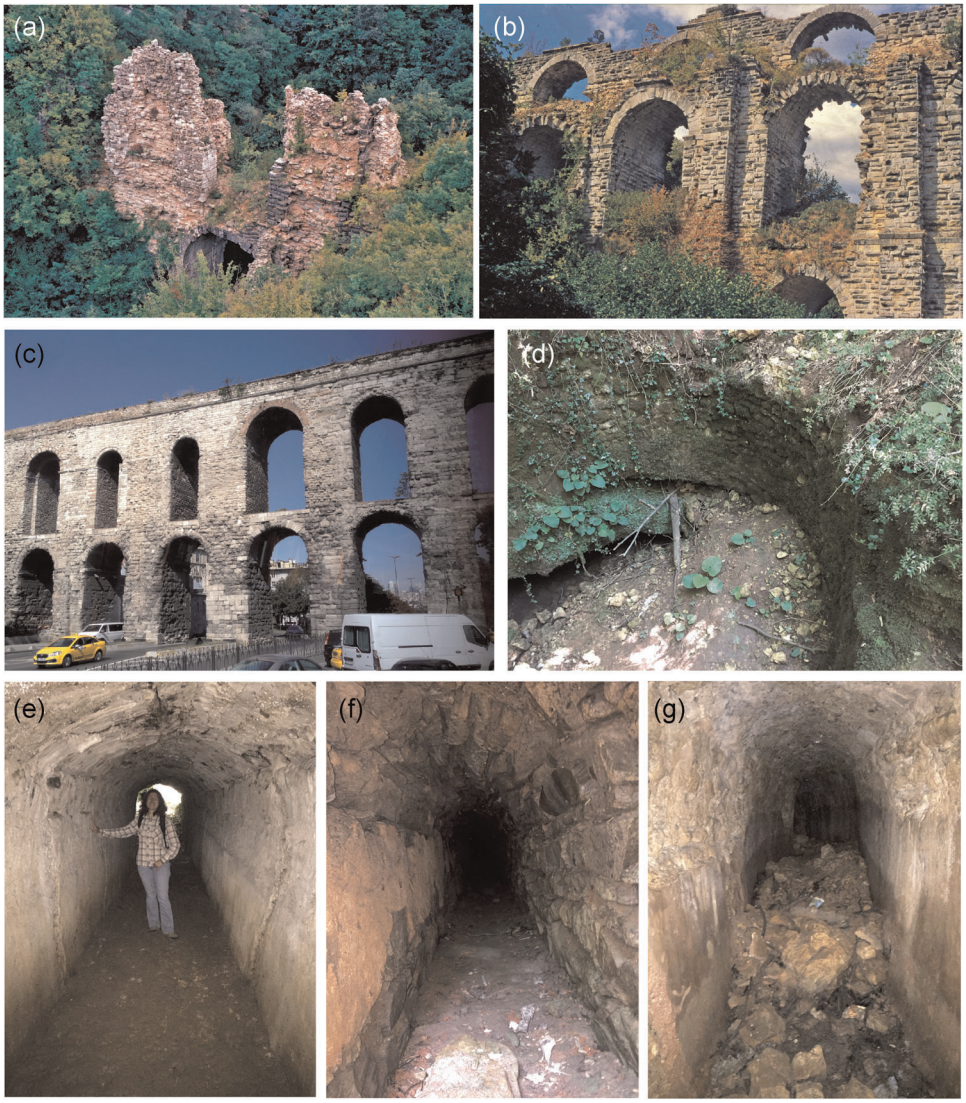

FIGURE 3 Remains of the Constantinople aqueducts. (a) Ballıgerme bridge before its destruction in 2020 in typical dense forest in Thrace, looking south; (b) Kurşunlugerme bridge looking west. The top two rows of arches carried the two water channels; (c) the Valens (Bozdoğankemer) aqueduct bridge in Istanbul, close to the end of the aqueduct; (d) one of the springs at Pınarca, dry when the photo was taken; (e) the wide channel of the fifth-century aqueduct at Ballıgerme; (f) the narrow channel of the fourth-century aqueduct near Kurşunlugerme bridge; (g) channel of the fourth-century Pınarca aqueduct branch close to the springs. Photos (a and b): J. Crow. (c–g): C. Passchier [Color figure can be viewed at wileyonlinelibrary.com]

Water samples were taken in June 2017 at the Pınarca and Pazarlı spring sites,[8] and stored in Teflon bottles for anion and cation analysis, and in glass bottles without ambient air for stable isotope analyses. Samples were analysed at the water laboratory of the Department of Earth Sciences, Mainz.

3 | RESULTS

3.1 | Macroscopic aspects of the samples

Carbonate samples were collected as a part of a separate fieldwork programme in 1999 at several sites along the aqueduct.[9]

[8]The Kaynarca and Paşa springs have not been investigated, as they were not accessible. The Kaynarca spring is also referred to as 'Danamandıra' in Ruggeri (2018). We do not use Danamandıra, because it is the name of a village close to both the Paşa and Kaynarca springs.

[9]Carbonate samples examined in this study were taken during field campaigns by Paolo Bono and Jim Crow in 1999. Locations are given in Figure 2 and some sampling sites are described in Crow et al. (2008) as follows: C1P—1.2, p. 31; C4A—1.5, p. 37; fig. 3.11 and p. 108; C6—1.4, p. 33; C5—1.7, p. 42 (G13).

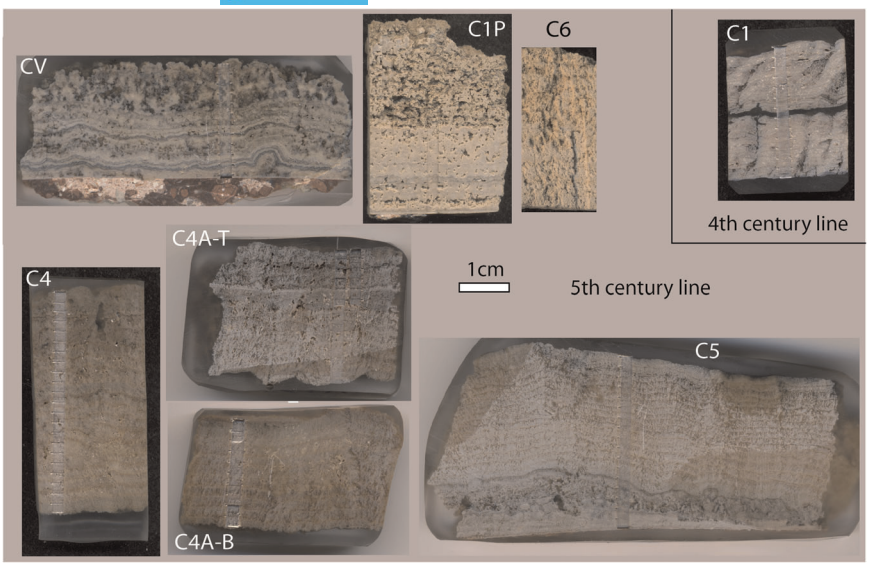

FIGURE 4 Cut carbonate samples from the aqueduct lines. Micromill traces for stable isotope analysis are visible on all samples as transects perpendicular to bedding. Photos: C. Passchier [Color figure can be viewed at wileyonlinelibrary.com]

The samples consist of two main groups: (1) carbonates of the fifth-century Pazarlı water supply: CV, C1P, C6, C4, C4A and C5; and (2) a single sample C1 from the fourth-century Pınarca water supply. The long-distance water supply lines were active until the 12th century (Crow et al., 2008; Ruggeri, 2018), and we suggest that carbonate found in-situ inside the channels dates back to this last period (Crow, 2019).

All samples are laminated in hand specimen and layering is particularly regular in samples C4 and C5 (Figure 4). Sample CV contains *opus signinum* from the inner face of the channel, but all other samples lack the plaster layer. However, since most samples have flat lower surfaces, they are considered to be (almost) complete, with possibly one to two layers missing at the bottom. Sample C4A was taken in two halves without stratigraphic interruption, labelled B (bottom) and T (top). C6 is relatively short, extremely porous and may be missing its top.

Several samples (CV, C1P, C6 and C4A) have enhanced porosity in the top layers, commonly after a sharp contact (Figure 4). Such a high porosity can be related to a change in the water composition, biological activity or, less commonly, diagenesis (Frisia, 2015; Pentecost, 2005). In C1P and C4A-T, the porous upper section is enriched in clay. After some years of carbonate precipitation, depositional conditions apparently changed, leading to the formation of porous carbonate at the top of the samples. The thickness of the carbonate stratigraphy in samples from different sampling locations is comparable. Samples CV, C1P and C5 show a similar stratigraphy in the lower part of the sample, with several porous layers, followed by a denser section and a dark band (Figure 4).

3.2 | Microfabrics

All samples are dominantly composed of micritic calcite (<4 μm; Boggs, 2011; Figures 4 and 5). The microfabric is layered but rather uniform, with a high porosity. The samples show similar features to riverine tufa deposits with a powdery brown porous structure, some with microbial filaments (Figure S1; Fairchild & Baker, 2012, Pedley & Rogerson, 2010). Micrite alternates with thin layers of microsparite, which has a larger crystal

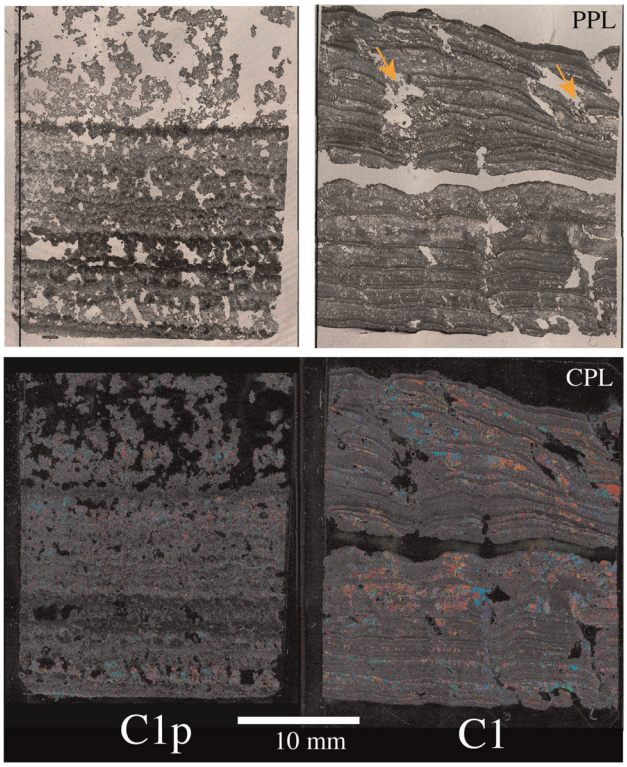

FIGURE 5 Microfabric of two representative samples, C1P and C1, obtained by Fabric Analyser G60 in plain polarised light (PPL) and cross-polarised light (CPL). The layering is an alternation of micrite (grey in CPL) and microsparite and sparite (bright colours in CPL). Ripple-like structures in C1 (arrows) indicate flow direction from right to left. Photos: M. Peternell [Color figure can be viewed at wileyonlinelibrary.com]

size (4–63 μm; Boggs, 2011; Figure 5). Layers of microsparite and sparite are mostly present in two samples, C1P and C1 (Figure 5). On the basis of macro- and microscopic observations, the following number of layers were counted: C6: 10–12; C4: 17–20; C4A: 24–27; C5: 20–25; C1: 14–20. C1, the only sample of the Pınarca spring, has the most regular stratigraphy. The sample shows rare ripple-like structures, similar to those in deposits of the Anio Novus aqueduct of Rome (Motta et al., 2017) and to 'crenulations'[10] commonly seen in cave deposits, especially in flowstones (Vesipa et al., 2015). The asymmetry of these ripple-like structures is shaped by the direction of water flow, with steep faces in the downstream direction. The ripple-like structures are partly separated by highly porous material, probably representing debris and biofilms concentrated in the troughs (Figure 5). A detailed description of the microstructure is given in the Supporting Information.

3.3 | Stable isotopes

Stable isotopes of oxygen ($\delta^{18}O$) and carbon ($\delta^{13}C$) were measured in all major samples along continuous tracks normal to the layering (Figure 6). The $\delta^{18}O$ signal is relatively flat in CV and C1P, close to the springs of the fifth-century channel, but it shows a clear cyclicity in downstream samples C6, C4, C4A and C5, which coincides with visible layering (Figure 6). The $\delta^{13}C$ signal is less pronounced, except for samples C4A and C5, and lacks the regular cyclicity seen in $\delta^{18}O$. In CV and C1P, the profile of $\delta^{13}C$ starts with elevated values and decreases gradually to a minimum, and in CV, it returns to the original values towards the end of the stratigraphy. There is an antithetic correlation between $\delta^{13}C$ and $\delta^{18}O$ for samples CV, C4, C4A-B and C5, but unusual covariance in parts of C4A-T and C6.[11] The top of sample C4A-T, which is enriched in clay, shows a distinct shift in the patterns of $\delta^{13}C$ and $\delta^{18}O$ (Figure 6, marked with an arrow). This clay-rich top layer is fragile and may have been lost in the other samples, because C4A has the largest number of documented layers of all samples. The mean value of $\delta^{18}O$ decreases with distance from the spring from −6.8‰ in CV to −7.5‰ in C5, whereas the mean value of $\delta^{13}C$ increases from −9.3‰ in CV to −8.8‰ in C5 (Figure 7).

C1, the only sample of the fourth-century line, differs from fifth-century line samples by the mean values and pronounced cyclicity of both $\delta^{13}C$ and $\delta^{18}O$ (Figures 6 and 7). Both stable isotopes show two trends: (1) a long-range trend of decreasing values, followed by an increase; (2) a pronounced, regular short-term cyclicity, where $\delta^{18}O$ cycles coincide with visible layering (Figure 6). The amplitude of $\delta^{13}C$ partly exceeds that of $\delta^{18}O$. C1 displays a visible covariance between $\delta^{18}O$ and $\delta^{13}C$.

3.4 | Trace elements

Minor and trace element analyses are commonly applied in palaeoenvironmental reconstructions of carbonate deposits (Fairchild & Baker, 2012; Pentecost, 2005). We measured short but distinct and representative sections to examine possible trends (Figure 6, green bars). The data presented here (Figure 8) are in the form of background-corrected counts for the different monitored isotopes, because the abundant presence of clay in the samples makes it impossible to apply a correct Ca content for each spot, which would be necessary to calculate element concentrations (Supporting Information). However, the basic count rates still allow a comparison of the relative abundance of elements in specific parts of the stratigraphy (Figure 8).

In most samples, peaks in ^{232}Th, ^{56}Fe, ^{27}Al, ^{139}La, ^{140}Ce, ^{141}Pr and ^{146}Nb coincide and correlate to some extent with increases in ^{24}Mg, ^{137}Ba, ^{86}Sr and ^{31}P (Figure 8). C4A-T shows a strong increase of several elements in the upper, porous and clay-rich part of the sample (Figure 8), probably reflecting the high clay content. For CV, only the bottom part of the sample including two dark layers was investigated and shows elevated levels of ^{86}Sr and ^{31}P. Sample C1 from the fourth-century channel has persistently high ^{43}Ca counts, suggesting rather clean and dense carbonate, with only a few thin laminae that are possibly enriched in clay. There is ^{86}Sr enrichment in the more compact layers that is well correlated with the high ^{43}Ca content of these layers.

3.5 | Microprobe observations—Presence of clay

Microprobe investigations of the porous top part of C4A-T (Figures 4 and 6) show high concentrations of Fe, Al, Si and K, confirming the presence of 20–30 vol% of clay minerals (Figure 9). A high porosity is visible in thin section (Figure 9a,b), but the pores may have contained clay that was partially removed during thin section preparation. The remaining clay is finely laminated, and the lamination is parallel to the outside of irregularly shaped carbonate particles, mantling the crystals (Figure 9c). Clay could have formed as a later infill after the channel stopped working, but in this case, it is hard to imagine how the fine and regular lamination formed. Therefore, it is more likely that clay was deposited while the aqueduct was functioning.

3.6 | Water analysis

Water samples of the springs of Pazarlı and Pınarca (Table 1) yielded similar mineral and stable isotope compositions, except for higher K, Sr and nitrate and lower Ca concentrations in Pazarlı.[12] High nitrate values are probably due to agricultural activity. The modern water of

[10]We prefer the term ripple-like structure over crenulation, due to the common use of the latter term to describe deformation features in structural geology.

[11]Correlation coefficients are as follows: C1 $r = 0.69$ (Pınarca); C1P $r = 0.62$ (Pazarlı); CV $r = -0.068$; C6 $r = 0.27$; C4 $r = -0.15$; C4 AB $r = -0.23$; C5 $r = -0.40$; C4AT $r = 0.50$.

[12]These values are confirmed in an unpublished report of Bono and Percopo (1998).

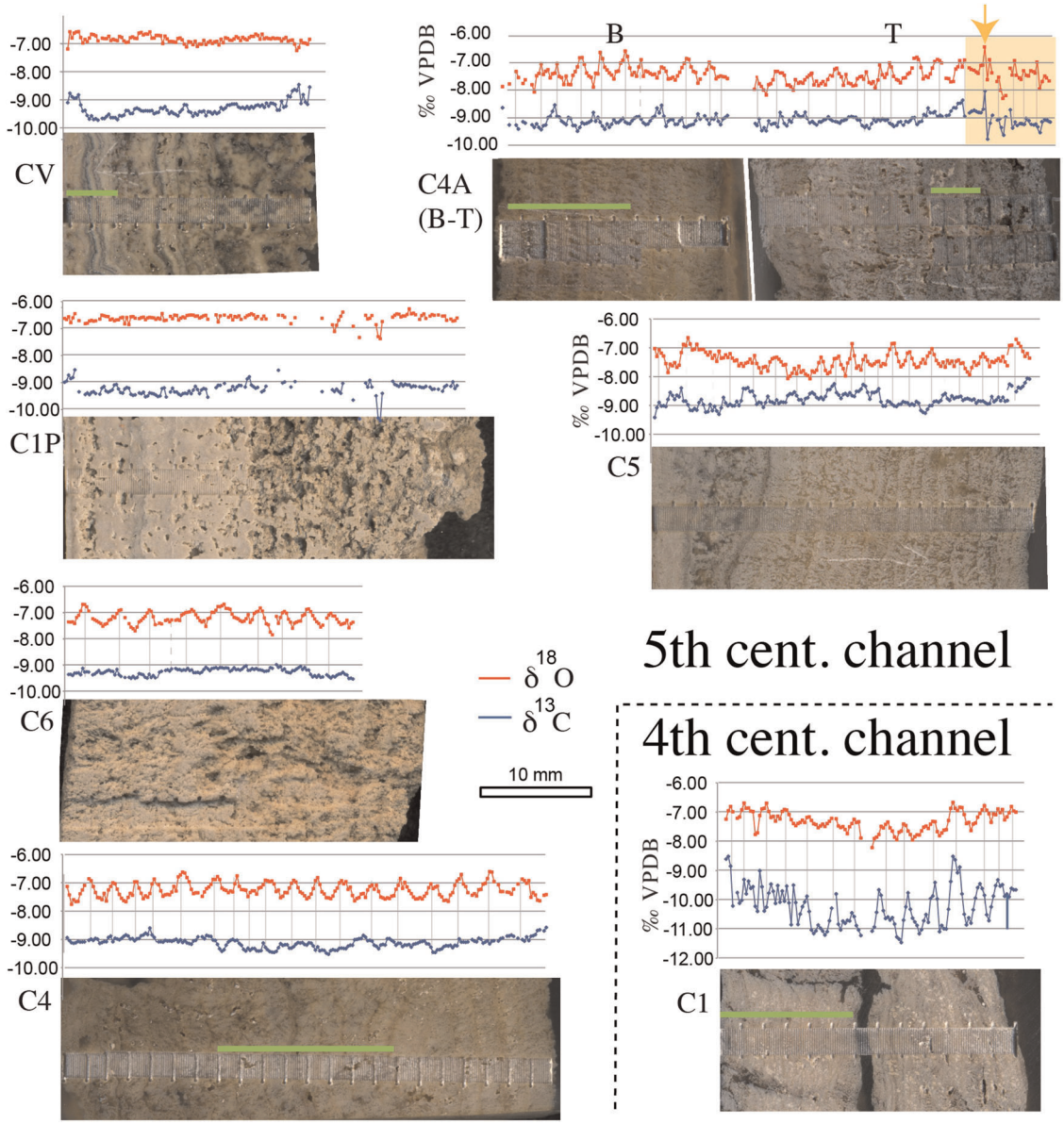

FIGURE 6 Stable isotope profiles with the micromilled sample slabs. Vertical bars in the diagrams indicate maxima of $\delta^{18}O$. Green bars on sample slabs indicate LA-ICP-MS traces of Figure 8. The orange marked area indicates the clay-rich top of C4A-T. The base of this clay rich area is separated by a grey layer from the rest of the stratigraphy. Orange arrow indicates a shift in stable isotope pattern within the clay rich top. Photos: C. Passchier [Color figure can be viewed at wileyonlinelibrary.com]

both springs is supersaturated with respect to calcite. Stable isotope values at Pınarca are slightly lower than those of Pazarlı.

4 | DISCUSSION

4.1 | Microfabrics

All samples show a dominance of dark micritic crystals and high porosity, with only a few layers of microsparite and sparite (Figures 4 and 5). The fine-crystalline and high-porosity fabric can be attributed to a relatively gentle slope and consequently slow water flow in the aqueduct (Passchier & Sürmelihindi, 2019).[13] Slow water flow promotes the growth of biofilms, which trap clay particles on their mucus surface and promote the nucleation of micrite crystals while preventing growth of larger, sparitic calcite crystals (Figures 5 and S1; Frisia, 2015; Sürmelihindi, Passchier, Baykan et al., 2013; Sürmelihindi, Passchier, Spötl et al., 2013; Wróblewski et al., 2017). Besides the biological content, enhanced supersaturation due to degassing may have also aided the formation of micrite. The high

[13]0.5–1.0 m/s (Ruggeri, 2018). Similar fabrics were found in other aqueducts with gentle slopes such as Ephesos (Passchier & Sürmelihindi, 2019), Saintes, Poitiers and Aix-en-Provence.

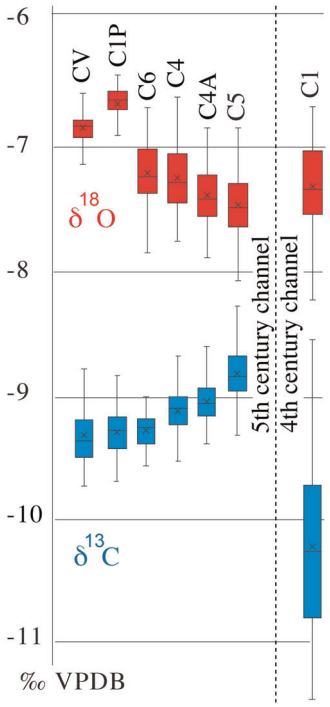

FIGURE 7 Box and whisker plots of stable isotope values for all samples. Both oxygen and carbon isotope values show a gradual change in downstream direction in the fifth-century channel [Color figure can be viewed at wileyonlinelibrary.com]

porosity may be due to the decay of biofilms. Some of the microsparites may have formed by crystal growth from original micrite (Frisia, 2015).

4.2 | Stable isotope composition

Annual cyclicity in $\delta^{18}O$ in aqueduct carbonate can be caused by seasonal variations in the composition and/or temperature of spring water (Stichler et al., 1997) or by evaporation or temperature changes in the aqueduct channel itself (Passchier, Sürmelihindi, & Spötl, 2016a; Passchier, Sürmelihindi, Spötl, Mertz-Kraus et al., 2016b, Passchier et al., 2020; Sürmelihindi, Passchier, Baykan et al., 2013; Sürmelihindi, Passchier, Spötl et al., 2013). In previous studies on ancient aqueduct settings from the Mediterranean realm, cyclical changes in $\delta^{18}O$ in aqueduct carbonate have been dominantly attributed to temperature-dependent isotope fractionation in response to seasonal temperature fluctuations of the aqueduct water (Benjelloun et al., 2019; Passchier, Sürmelihindi, & Spötl, 2016a; Passchier, Sürmelihindi, Spötl, Mertz-Kraus et al., 2016b; Passchier et al., 2020; Sürmelihindi, Passchier, Baykan et al., 2013; Sürmelihindi, Passchier, Spötl et al., 2013). High $\delta^{18}O$ values are perceived to indicate cold and wet conditions, whereas low values record calcite deposition during summer when temperatures were higher and discharge was lower (Passchier, Sürmelihindi, & Spötl, 2016a, Passchier et al., 2020; Sürmelihindi, Passchier, Baykan et al., 2013; Sürmelihindi, Passchier, Spötl et al., 2013).[14] $\delta^{18}O$ cyclicity, therefore, reveals the number of years an aqueduct was active, based on this seasonality, even though older carbonate deposits might have been removed.

$\delta^{13}C$ is usually affected by changes in vegetation cover, soil respiration, biological activity and degassing rate of CO_2 in the aqueduct channel (Baker et al., 1997; Baldini et al., 2005; Linge et al., 2001). The last two factors are directly related to discharge in the aqueduct (Sürmelihindi, Passchier, Baykan et al., 2013; Sürmelihindi, Passchier, Spötl et al., 2013). In carbonate deposits from aqueducts in the eastern Mediterranean, $\delta^{13}C$ commonly shows an antithetic cyclicity with $\delta^{18}O$. This was interpreted to reflect seasonal changes in discharge and water temperature (Passchier, Sürmelihindi, & Spötl, 2016a; Sürmelihindi, Passchier, Baykan et al., 2013), displaying the eastern Mediterranean climate with rainfall and high spring discharge during winter (Sürmelihindi, Passchier, Baykan et al., 2013; Sürmelihindi, Passchier, Spötl et al., 2013). In carbonate from western Mediterranean aqueducts, the $\delta^{13}C$ patterns are less bimodal and less pronounced due to the more homogeneous distribution of precipitation over the year and a less cyclic recharge of aquifers (Passchier, Sürmelihindi, & Spötl, 2016a).

Although the past cyclicity of water temperature and composition of aqueduct springs is unknown, it is possible to reconstruct these to some extent by comparison of upstream and downstream carbonate samples in aqueduct channels: upstream samples dominantly show the effect of the springs, whereas downstream ones show the combined effect of the springs and secondary effects which developed in the aqueduct channel such as evaporation, water temperature changes in response to air temperature changes and biological activity. $\delta^{18}O$ and $\delta^{13}C$ data in different samples along the aqueduct line allow to examine how the amplitude of the stable isotope profile changes in response to increasing distance from the source (Sürmelihindi, Passchier, Baykan et al., 2013). We were able to apply this technique to the fifth-century aqueduct (Figure 7).

4.3 | Pazarlı line—The fifth-century aqueduct

Modern data on the Pazarlı springs are limited (Crow et al., 2008, p. 52; Ruggeri, 2018, p. 156) and no monitoring data are available. However, the amplitude of $\delta^{18}O$ cyclicity in carbonate samples of the fifth-century aqueduct channel is very small in the upstream samples CV and C1P. This suggests that water $\delta^{18}O$ and temperature of these springs did not vary much over the year (Figure 6). This effect has been observed for fractured carbonate aquifers (Fairchild & Baker, 2012; Ford & Williams, 2007; Mook & Gat, 2001; Pentecost, 2005; Wang et al., 2020) and may apply to the Pazarlı aquifer. The amplitude of $\delta^{18}O$ cyclicity increases with distance from

[14]Aspendos and Patara in Turkey (Sürmelihindi, Passchier, Baykan et al., 2013; Sürmelihindi, Passchier, Spötl et al., 2013), Béziers, France (Passchier, Sürmelihindi, & Spötl, 2016a) and Jerash in Jordan (Passchier et al., 2020).

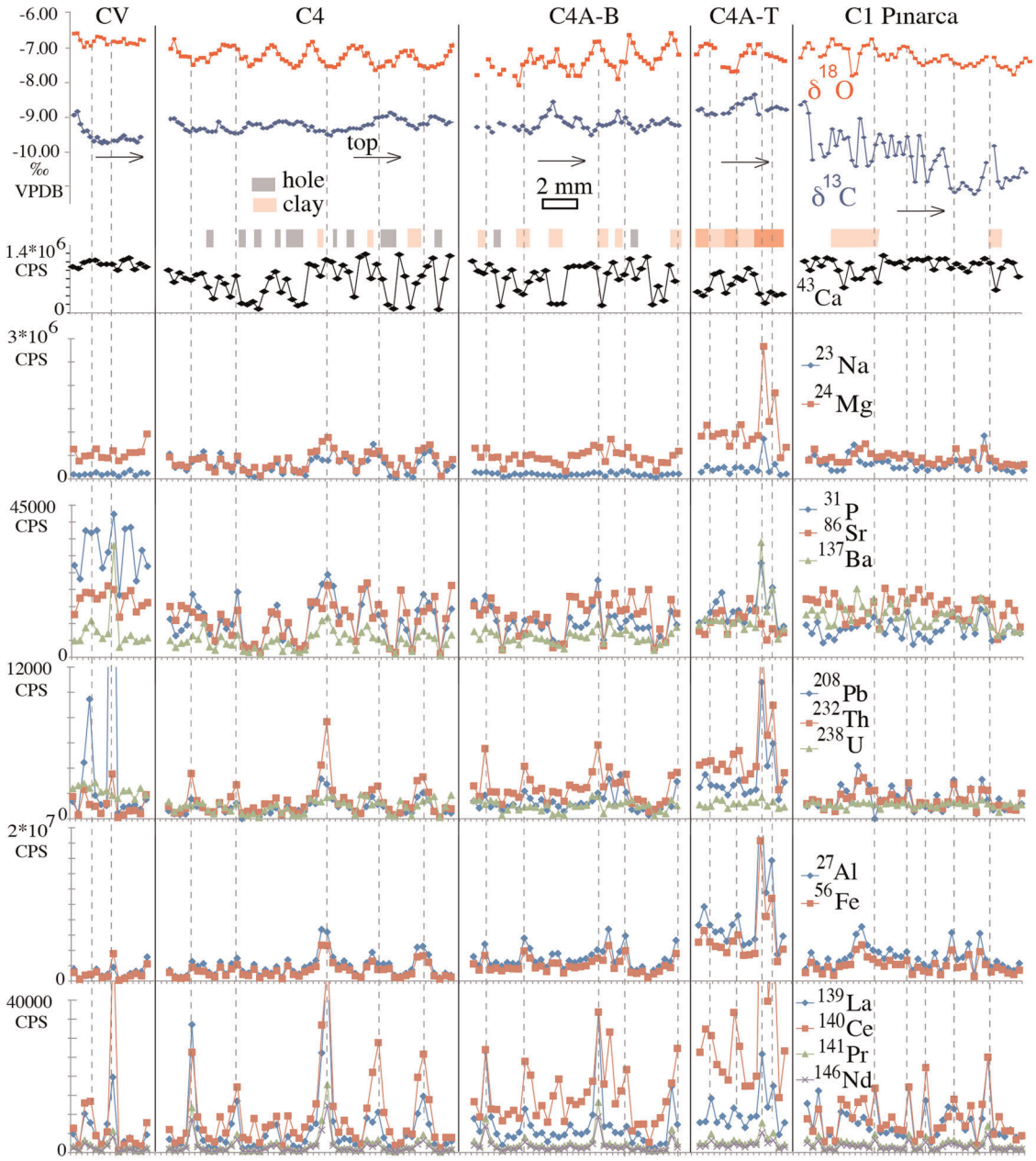

FIGURE 8 Trace element profiles of five samples along tracks shown in Figure 6. Profiles show raw count rates (counts per second [cps]) and have not been corrected to actual concentrations. Holes in porous parts of the samples are indicated by grey bars and high clay concentrations as pink bars at the top of the diagram. Stable isotope profiles are shown for correlation [Color figure can be viewed at wileyonlinelibrary.com]

the springs in samples C6, C4, C4A and C5 (Figure 6). The effects of the Ergene spring on these patterns is probably minor, because it only contributed 10%–20% of the water volume of the fifth-century channel (Ruggeri, 2018, p. 157) and both springs tap the same aquifer (Figure 2a; Bono et al., 2001). The cyclicity in $\delta^{18}O$ can, therefore, be attributed to evaporation and/or water temperature changes in the channel in response to seasonal changes in air temperature. Evaporation is not perceived to have had a dominant effect, because channels were closed and sealed by a vault, whereas the travelling time of water through the aqueduct was relatively short (<24 h from the spring to the sampling sites). Temperature-driven differences in near-equilibrium fractionation of oxygen isotopes could, therefore, have been the main driving factor for the observed cyclicity of $\delta^{18}O$ in downstream samples.

Cyclical variation in $\delta^{13}C$ in carbonate from other aqueducts has been attributed to a kinetic effect of variable degassing rates in response to seasonal variations in discharge and biological activity in the channel (Passchier, Sürmelihindi, & Spötl, 2016a; Passchier, Sürmelihindi, Spötl, Mertz-Kraus et al., 2016b; Sürmelihindi, Passchier, Baykan et al., 2013; Sürmelihindi, Passchier, Spötl et al., 2013).

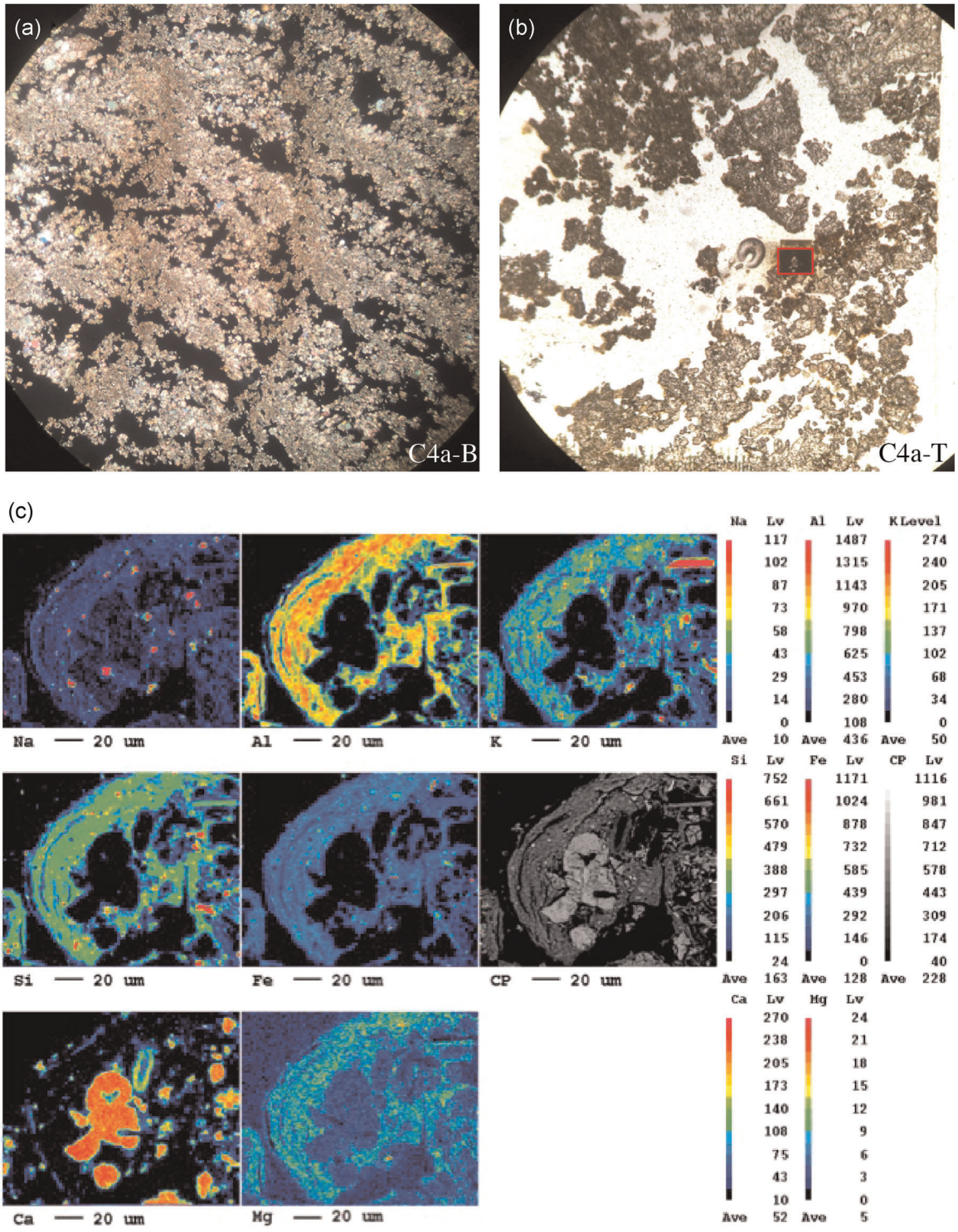

FIGURE 9 Thin section and microprobe images of C4A-B and -T. (a) A thin section image of porous carbonate in C4A-B. Width of view: 4 mm; (b) a thin section image of the top of C4A-T with clay-mantled carbonate. The red square indicates the area shown in c. Width of view: 2.5 mm; (c) microprobe analyses of carbonate grains, mantled by laminated clay. Photos (a and b): C. Passchier [Color figure can be viewed at wileyonlinelibrary.com]

TABLE 1 Composition of two springs of the aqueducts, sampled on 17 June 2017 at 41°16.374′ N, 028°19.126′ E (Pınarca) and 41°36.495′ N, 027°41.837′ E (Pazarlı)

Spring	*T* (°C)	Cond. (µS/cm)	pH	°dH	Na^+ (mg/L)	K^+ (mg/L)	Ca^{2+} (mg/L)	Mg^{2+} (mg/L)	Sr^{2+} (mg/L)	Ba^+ (mg/L)	Cl^- (mg/L)	NO_3^- (mg/L)	SO_4^{2-} (mg/L)	δD ‰	$\delta^{18}O$ ‰	$\delta^{13}C$ ‰
Pınarca	12.4	667	6.9	20	9.4	0.9	144.5	2.14	0.09	0.02	15.3	1.6	9.9	−52.9 ± 0.2	−8.6 ± 0.04	−15.9 ± 0.06
Pazarlı	15.4	563	7.3	14.4	10.4	1.9	111.6	3.35	0.16	0.02	17.3	13.6	8.8	−49.8 ± 0.4	−7.7 ± 0.08	−12.5 ± 0.07

Abbreviations: Cond., conductivity; °dH, degrees of German hardness.

In addition, this cyclical variation could be an effect of the source water reflecting seasonal variations in the contribution of soil-derived CO_2 to the dissolved inorganic carbon pool (Fairchild & Baker, 2012; Ford & Williams, 2007). This contribution is defined by variable discharge and residence times of water in the soil and aquifer that is directly controlled by rainfall patterns (Frisia et al., 2011; Passchier et al., 2020).

The $\delta^{13}C$ pattern in the fifth-century channel is relatively flat and irregular compared to that of eastern Mediterranean aqueducts, especially in upstream samples CV, C1P and C6, whereas the amplitude of variations in $\delta^{13}C$ increases downstream (Figure 6). This cannot be attributed to low resolution due to thin layering: in C6, the $\delta^{13}C$ curve is flat while $\delta^{18}O$ shows a clear cyclicity, and a weak $\delta^{13}C$ cyclicity is present in C4, C4A and C5 with similar layer thickness. Consequently, the variation in $\delta^{13}C$ of spring water of Pazarlı must have been minor and could reflect a relatively constant recharge of the aquifer over the year. Thrace, where the springs are located, is a transitional region between the Black Sea and Mediterranean climate, with rainfall more spread over the year than in the eastern Mediterranean. The observed variability in $\delta^{13}C$ in samples C4, C4A and C5, therefore, probably reflects downstream accumulating effects of seasonal fluctuations in water temperature and changes in discharge, causing variations in degassing and biological activity. Mean values of $\delta^{18}O$ in carbonate samples close to the springs are higher for Pazarlı (CV and C1P) than for Pınarca (C1), consistent with higher $\delta^{18}O$ values in Pazarlı spring water at present (Figure 7 and Table 1). The mean value of $\delta^{18}O$ in carbonate gradually decreases downstream, probably due to a gradual increase in mean annual water temperature downstream.[15] The mean value of $\delta^{13}C$ in carbonate increases downstream, probably due to preferential uptake of isotopically light carbon by biological activity (Mertz, 1992) and through degassing in the channel (e.g., Kele et al., 2011; Yan et al., 2020).

4.4 | Pınarca line—The fourth-century aqueduct

Sample C1, the only sample from the fourth-century channel, shows different stable isotope values and patterns compared to samples from the fifth-century line (Figures 6 and 7). Despite the fact that C1 was collected very close to the spring, it shows a pronounced cyclicity in both $\delta^{18}O$ and $\delta^{13}C$ with a clear covariation between the two isotopic values. Such covariation is rare in aqueduct carbonate elsewhere, whereas it is common in flowstones from caves (Polag et al., 2010; Wiedner et al., 2008). The strong cyclicity of $\delta^{18}O$ close to the spring suggests that this pattern may be diagnostic of the spring. In a large aquifer such as that of Pazarlı (Figure 2a), waters of different isotopic composition may mix before reaching the spring, cancelling out seasonal and short-term variations in $\delta^{18}O$, but in a small aquifer like Pınarca, the seasonal pattern may be preserved (Figure 2; Mook & Gat, 2001; Pentecost, 2005; Stichler et al., 1997).

Mean $\delta^{13}C$ is lower in C1 than in carbonate samples from the fifth-century channel deposits. At present, $\delta^{13}C$ in Pınarca spring water is also lower than in water of Pazarlı (Table 1), probably due to the dense cover of deciduous forest above the Pınarca aquifer (Figure 3a; Baldini et al., 2005; Fairchild & Baker, 2012). Relatively low $\delta^{13}C$ in C1 could reflect a similar local difference in vegetation cover in the Middle Ages. The observed $\delta^{13}C$ cyclicity in C1 is likely a kinetic effect of strong degassing due to a significant seasonal variation in discharge from a small aquifer, with minimum discharge in summer. Such variable discharge was reported for the springs of Danamandıra, which are fed by the same aquifer as the Pınarca spring (Bono et al., 2001; Crow et al., 2008, p. 52).

4.5 | Trace element data

In samples from the fifth-century channel such as C4A, cyclic peaks in ^{232}Th, ^{56}Fe, ^{27}Al, ^{139}La, ^{140}Ce and ^{146}Nd coincide with low ^{43}Ca count rates (Figure 8). This correlation suggests that these trace elements are linked with significant clay contamination (Figure 8). A link between element enrichment and high clay content was confirmed by microprobe analyses (Figure 9). Regular peaks in ^{232}Th, ^{139}La, ^{140}Ce and ^{146}Nd show an almost seasonal character (Figure 8). These peaks may be associated with colloids derived from the soil after heavy rainfall (Fairchild & Baker, 2012; Passchier, Sürmelihindi, & Spötl, 2016a). At the top of C4A-T, high values in most elements except ^{238}U and ^{86}Sr can be explained by a high clay content (Figures 8 and 9).

Sample C1 from the fourth-century channel shows low clay levels and low values of most trace elements, except near the base of the sample. However, ^{86}Sr is mimicking ^{43}Ca, probably reflecting compactness of the sample.

[15]The difference in $\delta^{18}O$ in Figure 7 between CV and C1P may be due to the fact that they are of different length and do not represent exactly the same stratigraphy.

4.6 | Clay in the channel

Our observations on carbonate deposits indicate that the aqueduct water in the represented period commonly carried a significant clay suspension load that left traces at several levels in the samples (C4 and particularly C4A; Figures 8 and 9). This may be partly due to the open intake structure of the Pazarlı water catchment and partly to the long sinuous nature of the fifth-century masonry channel (Figures 2a and 3a). Such a long, buried channel would inevitably have developed local damage by settling or tree roots, which would have been impossible to keep in constant repair. This could have caused contamination, for example, by storm water entering a damaged channel. The resulting suspension load of the water may be an additional reason for the presence of the large open Aetius, Aspar and Mocius reservoirs at the end of the aqueduct line. They served as storage basins, but also allowed clay particles to settle before water entered the city water supply network. The top of sample C4A-T differs from other sections by its exceptionally high clay content, above a sharp contact visible as a grey lamina in the sample (Figures 6 and 8). This implies a large amount of suspension in the channel during the last years of aqueduct operation.

4.7 | Carbonate thickness and cleaning

Generally, carbonate deposits in aqueduct channels are absent or thin near the spring, reach a maximum thickness at some distance from the spring, depending on supersaturation and degassing rate, and get thinner further downstream (Fabre et al., 2000; Sürmelihindi, Passchier, Baykan et al., 2013). This pattern is due to degassing of CO_2 from the water, leading to supersaturation and the onset of calcite deposition, followed by a decrease in deposition rate when CO_2 concentration in the water approaches equilibrium with atmospheric CO_2. The thickness of carbonate deposits and the fine- or coarse-crystalline nature of the fabric depends on the deposition rate as well as biological activity, with denser and coarser crystalline calcite being deposited in fast flowing water in the absence of biofilms (Passchier, Sürmelihindi, & Spötl, 2016a; Passchier et al., 2020; Sürmelihindi, Passchier, Baykan et al., 2013).

In the fifth-century line, samples CV and C1P close to the springs are laminated, whereas the rest of the samples show thicker layering. Only a very thin (1–2 mm) deposit of carbonate with fine laminae was observed at Ballıgerme in the fifth-century line, 180 km from the Pazarlı springs (Figure 2; Crow et al., 2008 p. 51). The carbonate deposition rate was apparently low at Ballıgerme, probably due to the considerable distance from the spring, where most carbonate had already precipitated upstream. Also, a few mm of carbonate was observed in the fourth-century upper channel at the Kurşunlugerme bridge, derived from the Danamandıra springs. C1 in the fourth-century line has relatively thicker layers; however, it is only at short distance from the spring of Pınarca (Figure 6). This can be attributed to a high mineralisation of the Pınarca spring water (Table 1) leading to a high carbonate deposition rate.

Microscopic and stable isotope observations confirm that none of our carbonate samples represent more than 27 years of deposition, as observed in sample C4A. Carbonate was deposited directly on the *opus signinum* lining of the channels and showed no sign of erosion or carbonate removal at the top of the deposits, indicating that the deposits represent less than three decades of aqueduct use. Compared with the 700 years of operation of the aqueduct, this number is very low. It implies that the studied deposits are the last to have formed in the channel during the Middle Ages, and that the older deposits had been removed from the aqueduct. This also explains the observation that not all samples can be correlated. The number of years represented by different samples differs even when compensating for possibly missing layers. The fifth-century channel at C6-C4-C4A-C5 may have been cleaned 25–27 years before the last use of the channel. Carbonate of the fourth-century channel at C1 shows between 14 and 20 years of deposition of unknown age (Figure 6). Again, this must be the last deposit in an aqueduct line that functioned over a long time and which had been cleaned at least 14 years before.

4.8 | Maintenance aspects

Historical sources mention that the combined fourth- and fifth-century aqueduct system was in use till the end of the 12th century, a period of more than 700 years. In the middle of the 12th century, Odo of Deuil described how freshwater flowed into the city in abundance (van der Vin, 1980)[16]; but less than 20 years later during a drought, Emperor Manuel I Komnenos (AD 1143–1180) ordered cleaning of the channels but felt unable to restore the old arcades (aqueduct bridges) which had decayed (Brand, 1976)[17]. From this comment, we can assume that at least the fifth-century channel in Thrace that carried water across large bridges such as Kurşunlugerme and Ballıgerme had ceased to function, providing a '*terminus ante quem*' for the last major maintenance and the build-up of carbonate and late clay deposits in that channel. The clay deposits at the top of sample C4A-T (Section 4.6; Figure 6) probably represent damage to the channel some years before final abandonment. Damage could have been caused by an earthquake or by the collapse of a section of aqueduct vault due to lack of maintenance. This dramatic event in the porous, clay-rich top of sample C4A-T is also indicated by a spike in $\delta^{18}O$ and $\delta^{13}C$, after which $\delta^{13}C$ shows a sudden drop (Figure 6, arrow). The final abandonment of the channel may have been due to an unrecorded earthquake or to collapse of one of the major bridges at the end of the 12th century.[18] Part of the fourth-century aqueduct may also still have functioned in the 12th century.

[16]Odo of Deuil. De profectione Ludovici VII in orientem. In van der Vin (1980).

[17]Ioannes Kinnamos, Deeds of John and Manuel Comnenos 6.8: 205-6; in Brand (1976).

[18]There are a number of historically attested earthquakes west of Constantinople in the 11th century in 1010,1037(?), 1038 (?), 1064 and 1081 (?), but there is a gap in the records between 1081 and 1202 (Downey, 1955). If there were local earthquakes in the 12th century, they did not leave records in the preserved literature. It seems likely that the aqueduct system was cumulatively damaged, not properly restored, and abandoned in the second half of the 12th century.

If the aqueducts had been cleaned shortly before they stopped operating, as suggested by the carbonate deposits, the question arises whether this was a regular process as *Frontinus* promoted more than a millennium earlier. Data sources for maintenance of the aqueduct system in the middle Byzantine period (9th–13th centuries) are virtually absent, but the aqueducts were certainly functioning around AD 1000 when there was evidence for repairs under Basil II at Ballıgerme with limited sources in the following century (Crow et al., 2008, p. 106). This implies that the city retained workers to ensure necessary repairs of the system as it did in the fifth century (Crow, 2012).

4.9 | The choice for a double-channel section

One of the intriguing aspects of the fourth- and fifth-century water supply system supporting Constantinople is the presence of an at least 50-km-long double-channel section, starting with a difference in elevation of 10 m at Ballıgerme and converging in elevation by Kalfaköy (Figures 2a, 10a and 10c). This section includes many parallel bridges and some large single bridges with two superposed channels (Figures 3b and 10c). At least some of these double-channel bridges, such as the Kurşunlugerme bridge (Figure 10e), replaced earlier single-channel bridges of the fourth-century channel, which were abandoned (Figure 10b). Also, many new bridges were built to cut-off loops into side valleys to shorten the length of the fourth-century channels (Crow, 2019). Since these new bridges were heavy constructions, some with pier diameters wider than the arches, anticipation of seismic damage may have been a driving factor to renew the bridges and build more massive piers (Figure 3a-c; Crow, in press). The question is, however, why a double channel was needed in this case.

One possible explanation is that the old channel was restored as an emergency channel in case of seismic damage. However, seismic damage could also occur outside the 50 km stretch of the double channel. Another possibility could be to use the old channel as a spare, to have enough capacity in times of high water demand. However, as the fifth-century channel arrived in Ballıgerme below the fourth-century channel and was of large dimensions (Figure 3e), it would have been possible to abandon the section of the fourth-century channel between Ballıgerme and Kalfaköy completely and divert all water from the Danamandıra springs into the new, larger channel (Figure 10d). Instead, the old fourth-century channel was restored and partly rerouted across new bridges to function together with and parallel to the new and wider fifth-century channel (Figure 10c). This reminds of the situation in Rome, where near-coinciding aqueducts of different age to the SE of the city were not merged into a single channel, but transported water separately to the city in two aqueduct lines with two (Aqua Claudia and Anio Novus) and three (Aqua Marcia, Tepula and Julia) stacked channels, respectively (Figure 10f,g; Aicher, 1995). The reasons to separate the channels in Rome were the different quality of water in the different

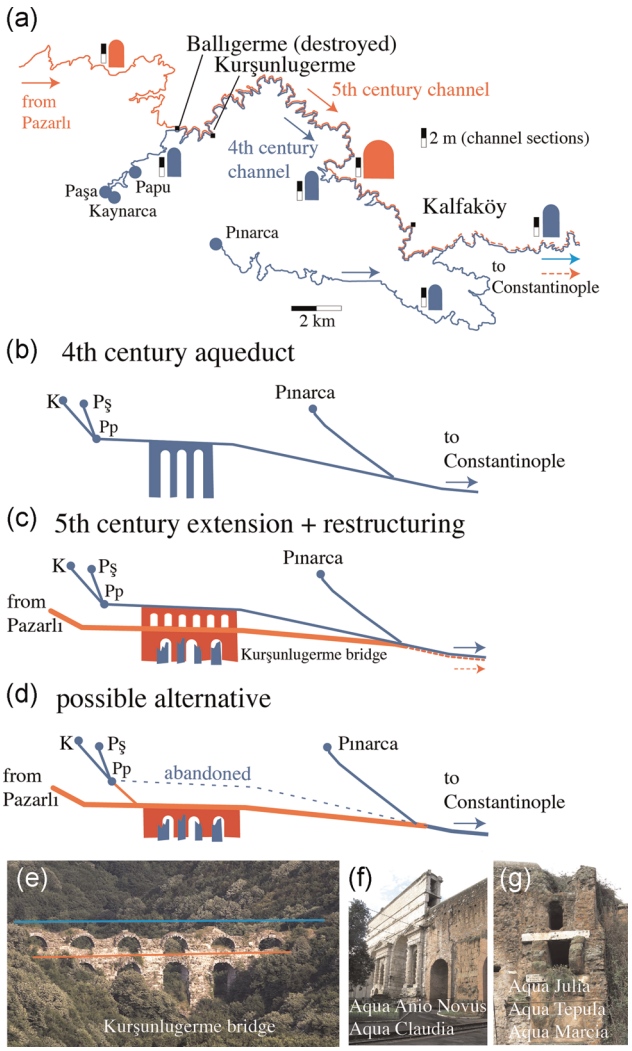

FIGURE 10 (a) map of the double-channel section. Representative channel profiles for each channel section are shown to scale. Scale bar = 2 m (after Ruggeri, 2018); (b) schematic presentation of the original single fourth-century channel layout; (c) addition of the fifth-century channel (red) and restructuring of bridges. Fourth-century bridges (blue) were replaced by massive new bridges (red) to prevent seismic damage. Some bridges carry two channels. It is uncertain if the fifth-century channel extended to the city; (d) a simpler alternative setting, which was not built, where a single new channel carries all the water. (b–d) not to scale. K, Pş and Pp refer to the names of springs in (a); (e) Kurşunlugerme bridge with the two water channels; (f and g) superimposed channels of the Roman aqueducts at Porta Maggiore in Rome, for comparison. Photo (e): J. Crow. (f and g): C. Passchier [Color figure can be viewed at wileyonlinelibrary.com]

channels and ease of maintenance for repairs and removal of carbonate, with the option to temporary cut-off certain channels without interrupting the entire water supply (Aicher, 1995). Similar reasons could have applied for the double-channel arrangement for Constantinople. Trace element analysis suggests that water of the

fifth-century channel was commonly contaminated with clay, which could be one reason to keep this water separated from that of the fourth-century channel. This only applies, however, if water was kept separated all the way to the city. If there was only one channel downstream from Kalfaköy, the enabling of maintenance must have been the driving factor to build a double channel.

As up to 27 years of carbonate deposits were preserved in the channels, the aqueduct had been previously cleaned, possibly as part of a regular maintenance cycle. Due to the length of the channel, such a cleaning and maintenance operation might have lasted several months, even with a large crew. The channels probably had to be closed for this work. Since carbonate deposition is most pronounced at some distance from the springs, the two branches of the fourth-century aqueduct and the upper part of the fifth-century channel needed regular cleaning, besides other maintenance operations. This could be done by closing the fifth-century channel alternating with the two upper branches of the fourth-century one (Figure 10c). Such a system of operation could have provided a permanent water supply. The costly 50-km-long double-channel system may, therefore, have been set up for the purpose of maintenance and carbonate removal and the provision of a continuous water supply.[19]

Our observations on carbonate forming in the Constantinople water supply are also relevant for the question why the system was built and extended the way it was. Constantinople was located in a unique geographical position at the end of a long and rather low-lying peninsula, restricting potential freshwater sources (Bono et al., 2001). The aqueduct system was probably extended with the Pazarlı branch in the fifth century because of increasing demand due to population rise and because of failure in discharge of the Pınarca spring due to its small aquifer. The Danamandıra and Pınarca springs may have fallen dry during long-lasting droughts, and this may have been an additional incentive to build the much longer and no doubt costly fifth-century branch extension all the way from Pazarlı.

5 | CONCLUSIONS

- Carbonate deposits in the fifth-century aqueduct of Constantinople represent a maximum of 27 years of deposition during the last decades of activity of the water supply system in the late 12th century. Since the aqueduct was in use for several centuries, this implies that the channel was cleaned, possibly regularly. The fourth-century branch contains at least 14 years of carbonate from the same period.
- $\delta^{18}O$ shows a regular cyclicity, probably in response to seasonal temperature changes in the long aqueduct channel. This cyclicity allows counting of annual layers.
- $\delta^{13}C$ and $\delta^{18}O$ profiles in the fifth-century channel carbonates show only a weak and variable correlation, probably in response to evenly distributed rainfall over the year in the Thrace area.
- The $\delta^{13}C$ and $\delta^{18}O$ profiles of carbonate from the fourth-century channel show covariance and therefore differ significantly from stable isotope profiles of the fifth-century channel. They possibly reflect seasonal variations in discharge and $\delta^{18}O$ of the spring water. The difference can be attributed to the smaller size of the aquifer of the fourth-century channel compared to that of the fifth-century one.
- Water in the fifth-century channel was commonly contaminated with clay. The large strategic open water storage basins of Aetius, Aspar and Mocius in Constantinople may have had the additional function to allow clay particles to settle down.
- The double section of the fourth- and fifth-century channels may have been built to allow cleaning and repair of one branch while the other one remained in operation, in anticipation of the long time needed for cleaning operations.

[19]As an additional tool, dropshafts may have connected the double channels between Ballıgerme and Kalfaköy, as in Rome for the Aqua Marcia and Anio Vetus.

ACKNOWLEDGEMENTS

Samples for this study were provided to the authors by Prof. Paolo Bono of Sapienza University, Rome, on 8 January 2010. Prof. Bono obtained the samples as part of his collaboration with Prof. Jim Crow who directed the Water Supply of Constantinople Project (1998–2004) funded by the Leverhulme Research Trust and the AHRC. Prof. Bono passed away in 2012 before the authors could analyse the samples, and this paper is dedicated to his memory. The current programme of analysis was conducted as part of the project 'Engineering the Water Supply of Byzantine Constantinople', funded by the Leverhulme Research Trust RPG-2013-410 (2014–2017). This programme was also supported by DFG projects PA578/17 and SU864/2-1. Authors thank Mark Peternell for photographing samples with the Fabric Analyser and Nora Groschopf for microprobe analysis. Open Access funding enabled and organized by Projekt DEAL.

CONFLICT OF INTERESTS

The authors declare that there are no conflicts of interest.

PEER REVIEW

The peer review history for this article is available at https://publons.com/publon/10.1002/gea.21853

DATA AVAILABILITY STATEMENT

Data are available from the corresponding author on request.

ORCID

Gül Sürmelihindi http://orcid.org/0000-0001-7874-8631
Cees Passchier https://orcid.org/0000-0002-3685-7255
James Crow https://orcid.org/0000-0002-9478-973X
Christoph Spötl https://orcid.org/0000-0001-7167-4940
Regina Mertz-Kraus https://orcid.org/0000-0002-5122-4480

REFERENCES

Aicher, P. J. (1995). *Guide to the aqueducts of ancient Rome*. Bolchazy-Carducci Publishers.

Baker, A., Ito, E., Smart, P. L., & McEwan, R. F. (1997). Elevated and variable values of ^{13}C in speleothems in a British cave system. *Chemical Geology*, *136*, 263–270. https://doi.org/10.1016/S0009-2541(96)00129-5

Baldini, J. U. L., McDermott, F., Baker, A., Baldini, L. M., Mattey, D. P., & Bruce Railsback, L. (2005). Biomass effects on stalagmite growth and isotope ratios: A 20th century analogue from Wiltshire, England. *Earth and Planetary Science Letters*, *240*, 486–494. https://doi.org/10.1016/j.epsl.2005.09.022

Benjelloun, Y., Carlut, J., Hélie, J.-F., Chazot, G., & Callonnec, L. (2019). Geochemical study of carbonate concretions from the aqueduct of Nîmes. *Scientific Reports*, *9*, 5209. https://doi.org/10.1038/s41598-019-41620-4

Boggs, S., Jr. (2011). *Principles of sedimentology and stratigraphy*. Pearson Prentice Hall.

Bono, P., Crow, J., & Bayliss, R. (2001). The water supply of Constantinople: archaeology and hydrogeology of an early Medieval city. *Environmental Geology*, *40*, 1325–1333. https://doi.org/10.1007/s002540100365

Bono, P., & Percopo, C. (1998). *L'acquedotto di Valente: Contributo dell'idrogeologia alla ricerca archeologica (campagna 1998)* (Internal Report).

Brand, C. (1976). *Deeds of John and Manuel Comnenus by John Kinnamos*. Columbia University Press.

Çeçen, K. (1996). *The longest Roman water supply line*. Türkiye Sınai Kalkınma Bankası.

Crow, J. (2012). Ruling the waters: Managing the water supply of Constantinople, AD 330-1204. *Water History*, *4*, 35–55. https://doi.org/10.1007/s12685-012-0054-y

Crow, J. (in press). Bridges on the longest Roman water supply line. In G. Fingarova & A. Kulzer, A. (Eds.), *Crossing rivers in Bryzantium and beyond: Historical studies in historical geography and cultural heritage* (Vienna and Novi Sad).

Crow, J. (2019). The imagined water supply of Byzantine Constantinople, new approaches. *Traveaux et Mémoires*, *22*, 211–235.

Crow, J., Bardill, J., & Bayliss, R. (2008). *The water supply of Byzantine Constantinople* (Vol. 11). Society for the Promotion of Roman Studies.

Downey, G. (1955). Earthquakes at Constantinople and Vicinity, A.D. 342-1454. *Speculum*, *30*, 596–600.

Fabre, G., Fiches, J.-L., Paillet, J.-L., & Pey, J. (2000). Le trace de l'aqueduc dans son environnement. In G. Fabre, J.-L. Fiches, & J.-L. Paillet (Eds.), *L'aqueduc de Nîmes et le Pont du Gard* (pp. 57–121). CNRS Editions.

Fairchild, I. J., & Baker, A. (2012). *Speleothem science*. Wiley-Blackwell.

Ford, D. C., & Williams, P. (2007). *Karst hydrogeology and geomorphology*. John Wiley & Sons.

Frisia, S. (2015). Microstratigraphic logging of calcite fabrics in speleothems as tool for palaeoclimate studies. *International Journal of Speleology*, *44*, 1–16. https://doi.org/10.5038/1827-806X.44.1.1

Frisia, S., Fairchild, I. J., Fohlmeister, J., Miorandi, R., Spötl, C., & Borsato, A. (2011). Carbon mass-balance modelling and carbon isotope exchange processes in dynamic caves. *Geochimica et Cosmochimica Acta*, *75*, 380–400.

Hodge, A. T. (2011). *Roman aqueducts and water supply* (2nd ed.). Bloomsbury Academic.

Kele, S., Özkul, M., Fórizs, I., Gökgöz, A., Baykara, M. O., Alçiçek, M. C., & Németh, T. (2011). Stable isotope geochemical study of Pamukkale travertines: New evidences of low-temperature non-equilibrium calcite-water fractionation. *Sedimentary Geology*, *238*, 191–212.

Kienast, H. (1995). Die Wasserleitung des Eupalinos auf Samos, *Deutsches Archaeologisches Institut: Samos Band XIX* (p. 229). Rudolf Habelt.

Linge, H., Lauritzen, S.-E., Lundberg, J., & Berstad, I. M. (2001). Stable isotope stratigraphy of Holocene speleothems: examples from a cave system in Rana, northern Norway. *Paleogeography, Paleoclimatology, Paleoecology*, *167*, 209–224. https://doi.org/10.1016/S0031-0182(00)00225-X

Lom, N., Ülgen, S. C., Sakınç, M., & Şengör, A. M. C. (2016). Geology and stratigraphy of Istanbul region. *Geodiversitas*, *38*, 175–195.

Mango, C. (1995). The water supply of Constantinople. In C. Mango, G. Dagron, & G. Greatrex (Eds.), *Constantinople and its Hinterland: Papers from the Twenty-Seventh Symposium of Byzantine Studies* (pp. 9–18). CRC Press.

Mango, C., & Scott, R. (1997). *The chronicle of Theophanes Confessor: Byzantine and near Eastern History AD 284-813*. Clarendon Press.

Matias Rodrigues, R. (2017). Las Medulas: Revision e incognitas sobre la tecnologia minera romana de la mayor explotacion del mundo antiguo. *Actas del XI Congreso Internacional de Historia de la Mineria*, 235–244.

Mertz, M. U. E. (1992). The biology of carbonate precipitation by cyanobacteria. *Facies*, *26*, 81–101.

Mook, W. G., & Gat, J. R. (2001). Environmental isotopes in the hydrological cycle: principles and applications, *Agencia Internacional de Energía Atómica*. Environmental Science.

Motta, D., Keenan-Jones, D., Garcia, M. H., & Fouke, B. W. (2017). Hydraulic evaluation of the design and operation of ancient Rome's Anio Novus aqueduct. *Archaeometry*, *59*, 1150–1174. https://doi.org/10.1111/arcm.12303

Oleson, J. P. (1984). *Greek and Roman mechanical water-lifting devices: The history of a technology*. Springer.

Passchier, C., Rigal, D., & Sürmelihindi, G. (2015). Preuves du nettoyage des concrétions calcaires de l'aqueduc antique de Divona-Cahors. Aquae ductus. *Aquitania Supplement*, *33*, 233–241.

Passchier, C., Sürmelihindi, G., & Spötl, C. (2016a). A high-resolution palaeoenvironmental record from carbonate deposits in the Roman aqueduct of Patara, SW Turkey, from the time of Nero. *Scientific Reports*, *6*, 28704. https://doi.org/10.1038/srep28704

Passchier, C., Sürmelihindi, G., Spötl, C., Mertz-Kraus, R., & Scholz, D. (2016b). Carbonate deposits from the ancient aqueduct of Béziers, France—A high-resolution palaeoenvironmental archive for the Roman Empire. *Palaeogeography, Palaeoclimatology, Palaeoecology*, *461*, 328–340. https://doi.org/10.1016/j.palaeo.2016.08.022

Passchier, C. W., & Sürmelihindi, G. (2019). Carbonate deposits of the Değirmendere Aqueduct. In G. Wiplinger (Ed.), *Der Değirmendere Aquädukt von Ephesos* (Vol. 36, pp. 511–522). Babesch Supplements.

Passchier, C. W., Sürmelihindi, G., Boyer, D., Yalçın, Ç., Spötl, C., & Mertz-Kraus, R. (2020). The aqueduct of Gerasa—Intra-annual palaeoenvironmental data from Roman Jordan using carbonate deposits. *Palaeogeography, Palaeoclimatology, Palaeoecology*, *562*, 110089. https://doi.org/10.1016/j.palaeo.2020.110089

Pedley, H. M. & Rogerson, M., (eds). (2010). *Tufas and speleothems: Unravelling the microbial and physical controls* (p. 336). Geological Society of London.

Pentecost, A. (2005). *Travertine*. Springer.

Peternell, M., Kohlmann, F., Wilson, C. J. L., Seiler, C., & Gleadow, A. J. W. (2009). A new approach to crystallographic orientation measurement for apatite fission track analysis: Effects of crystal morphology and implications for automation. *Chemical Geology*, *265*, 527–539. https://doi.org/10.1016/j.chemgeo.2009.05.021

Polag, D., Scholz, D., Mühlinghaus, C., Spötl, C., Schröder-Ritzrau, A., Segl, M., & Mangini, A. (2010). Stable isotope fractionation in speleothems: Laboratory experiments. *Chemical Geology*, *279*(1-2), 31–39. https://doi.org/10.1016/j.chemgeo.2010.09.016

Ruggeri, F. (2018). *Engineering the Byzantine Water Supply of Constantinople: mapping, hydrology and hydraulics of the long aqueducts outside the City* (PhD thesis). University of Edinburgh, Edinburgh.

Snyder, J. R. (2012). *Construction requirements of the water supply of Constantinople and Anastasian wall* (PhD thesis). University of Edinburgh, Edinburgh.

Spötl, C., & Vennemann, T. W. (2003). Continuous-flow isotope ratio mass spectrometric analysis of carbonate minerals. *Rapid Communications*

in Mass Spectrometry, *17*, 1004–1006. https://doi.org/10.1002/rcm.1010

Stichler, W., Trimborn, P., Maloszewski, P., Rank, D., Papesch, W., & Reichert, B. (1997). 5.1. Environmental isotope investigations. In F. Cicchi, J. Car, I. Gams (Eds.), Karst hydrogeological investigations in south-western Slovenia (Vol. 26, pp. 213–235). Acta Carsologica.

Sürmelihindi, G., Passchier, C. W., Baykan, O. N., Spötl, C., & Kessener, P. (2013). Environmental and depositional controls on laminated freshwater carbonates: An example from the Roman aqueduct of Patara, Turkey. *Palaeogeography, Palaeoclimatology, Palaeoecology*, *386*, 321–335. https://doi.org/10.1016/j.palaeo.2013.06.002

Sürmelihindi, G., Passchier, C. W., Leveau, P., Spötl, C., Bourgeois, M., & Bernard, V. (2019). Reconstructing the hydraulics of the world's first industrial complex using carbonate deposits—The Barbegal watermills, France. *Journal of Archaeological Science: Reports*, *24*, 1041–1058.

Sürmelihindi, G., Passchier, C. W., Spötl, C., Kessener, P., Bestmann, M., Jacob, D. E., & Baykan, O. N. (2013). Laminated carbonate deposits in Roman aqueducts: Origin, processes and implications. *Sedimentology*, *60*, 961–982. https://doi.org/10.1111/sed.12000

Türkecan, A., & Yurtsever, A. (2002). *Geological map of Turkey (1:500.000)*. General Directorate of Mineral Research and Exploration.

Varol, B., Baykal, M., & Ayyıldız, T. (2009). Sedimentological-stratigraphical evaluation of tertiary carbonates (Soğucak formation) of Thrace Basin (Bozcaada-Kiyiköy). *Bulletin of the Mineral Research and Exploration*, *139*, 1–15.

Vesipa, R., Camporeale, C., & Ridolfi, L. (2015). Thin-film-induced morphological instabilities over calcite surfaces. *Proceedings of the Royal Society A*, *471*, 20150031. https://doi.org/10.1098/rspa.2015.0031

van der Vin, J. P. (1980). *Travellers to Greece and Constantinople: Ancient monuments and old traditions in medieval travellers' tales* (p. 49). Leiden, PIHANS.

Wang, F., Chen, H., Lian, J., Fu, Z., & Nie, Y. (2020). Seasonal recharge of spring and stream waters in a karst catchment revealed by isotopic and hydrochemical analyses. *Journal of Hydrology*, *591*, 125595.

Ward, K. A., Crapper, M., Altug, K., & Crow, J. (2017). The Byzantine cisterns of Constantinople. *Water Science and Technology: Water Supply*, *17*, 1499–1506. https://doi.org/10.2166/ws.2017.053

Wiedner, E., Scholz, D., Mangini, A., Polag, D., Mühlinghaus, C., & Segl, M. (2008). Investigation of the stable isotope fractionation in speleothems with laboratory experiments. *Quaternary International*, *187*(1), 15–24. https://doi.org/10.1016/j.quaint.2007.03.017

Wróblewski, W., Gradziński, M., Motyka, J., & Stankovič, J. (2017). Recently growing subaqueous flowstones: Occurrence, petrography and growth conditions. *Quaternary International*, *437*, 84–97.

Yan, H., Liu, Z., & Sun, H. (2020). Large degrees of carbon isotope disequilibrium during precipitation-associated degassing of CO_2 in a mountain stream. *Geochimica et Cosmochimica Acta*, *273*, 244–256.

SUPPORTING INFORMATION

Additional Supporting Information may be found online in the supporting information tab for this article.

How to cite this article: Sürmelihindi, G., Passchier, C., Crow, J., Spötl, C., & Mertz-Kraus, R. (2021). Carbonates from the ancient world's longest aqueduct: A testament of Byzantine water management. *Geoarchaeology*, 1–17. https://doi.org/10.1002/gea.21853